Harmonics and interharmonics compensation with active front-end converters based only on local voltage measurements

D'Arco, Salvatore; Ochoa-Gimenez, Miguel; Piegari, Luigi; Tricoli, Pietro

DOI:
10.1109/TIE.2016.2588462

Harmonics and Inter-Harmonics Compensation with Active Front-End Converters Based only on Local Voltage Measurements

Salvatore D'Arco, Miguel Ochoa-Gimenez, Luigi Piegari, *Senior Member, IEEE* and Pietro Tricoli, *Member, IEEE*

***Abstract*— The current grid codes for distribution networks impose on operators to provide ancillary services, like fault ride through capability and reactive power compensation. In this context, generating units with power electronics interfaces could offer as an additional service the active compensation for harmonic and inter-harmonic currents introduced by other converters or distorting loads. Typically, the converters of these generating units do not have information on the distortion of either other loads or of the grid current. Thus, this paper presents a control algorithm for grid harmonics and inter-harmonics compensation that relies only on the measurement of the voltage at the point of connection of the unit. The reference for the compensating current is calculated from the harmonic components of grid voltage in the synchronous reference frame. The paper also addresses the influence on the compensation performance of the line impedance between the generating unit and the point of connection. Experimental tests on a laboratory setup fully validate the proposed compensation method.**

***Index Terms*— Active filters, distributed generation, inter-harmonic compensation, multiple-reference-frame.**

I. Introduction

NOWADAYS grid-tie converters are widely used in industrial, commercial, and domestic applications. Examples include electrical drives, DC power supplies, uninterruptible power supplies, power conditioners and active front-end converters for renewable energy sources (RES) and storage devices. Although present standards impose limits on the magnitude of harmonic currents injected into the grid [1], a large number of power converters can distort the voltage at the point of common coupling (PCC), particularly for weak grids, like rural networks [2]-[3], or for resonant conditions [4]-[5].

In recent years, several European and American distribution system operators (DSO) have defined grid codes for the connection of distributed generators (DG) to the AC distribution networks [6]. In some countries, these codes have been developed specifically for the distribution networks, while in other countries they have been integrated with the grid codes for the connection to the transmission system. The grid codes of 7 countries and 2 standards (ENTSO-E and IEEE 1547) require grid-tie converters for RES to provide ancillary services [6]. Typical steady-state requirements are: frequency and voltage monitoring, active power control and reactive power control; typical transient requirements are: grid voltage support during disturbances, reactive current regulation for fast voltage control, inertia emulation, and damping.

Some of these ancillary services are mandatory while others are remunerated. The increasing level of the harmonic pollution suggests a future scenario where some DSOs could remunerate the harmonic filtering service. Therefore, RES with grid-tie converters operating at sufficiently high switching frequencies (5-10 kHz) could provide active filtering services and some examples of this have been already presented in the technical literature [7]-[8].

Active filtering decreases the maximum active power that can be generated by the RES. However, the power necessary for active filtering can be maintained at a very low level with an accurate design of the control and of the passive components. For example, in [9] the power usage of the active filter is about 1.5% of the nominal value. For the specific case of RES, the reduction of actual power generated might be negligible in practice, because RES operate at nominal power only for a limited period of time per day. For example, the typical capacity factor is about 12-15% for photovoltaic arrays and 20-40% for wind turbines [10]. When the converter does not operate at its nominal power, the active filtering service could be an extra source of income for DSOs at the price of

Manuscript received September 4, 2015; revised March 7, 2016 and May 11, 2016; accepted June 6, 2016. This work was supported in part by the EU FP7 Marinet Project. The work of M. Ochoa-Gimenez is partially financed by the Spanish Government through grant ENE2011-28527-C04-01 and BES-2012-055790.

S. D'Arco is with Electric Power Systems Department, SINTEF Energy Reearch A.S, Trondheim, Norway (e-mail: Salvatore.darco@sintef.no).

M. Ochoa-Gimenez is with Gamesa Electric in Madrid, Spain. His areas of interest are FACTS, Madrid, Spain (e-mail: MOCHOA@gamesacorp.com).

L. Piegari is with the Department of Electronics, Information and Bioengineering (DEIB) of the Politecnico di Milano, Piazza Leonardo da Vinci 32, I 20133 Milan, Italy (email: luigi.piegari@polimi.it).

P. Tricoli is with the Department of Electronic, Electrical and Systems Engineering, University of Birmingham, Birmingham, B15 2TT, UK (e-mail: p.tricoli@bham.ac.uk).

This article has been accepted for publication in a future issue of this journal, but has not been fully edited. Content may change prior to final publication. Citation information: DOI 10.1109/TIE.2016.2588462, IEEE Transactions on Industrial Electronics

additional operating losses. Moreover, this service could spare DSOs the installation of harmonic filters on the distribution network.

Grid-tie converters for RES providing filtering services operate in a way similar to active power filters (APFs), although they have a fundamental harmonic of the current that follows the active power generated by the RES. The basic principle of APFs was originally presented back in 1971 [11]. Since then, many different control schemes have been proposed to compensate for grid harmonics [12]. At the present state of the art, these schemes can be mainly classified into three different groups: methods based on the measurement of the instantaneous power, methods based on the measurement of the current and methods based on the measurement of the voltage at the PCC. The main disadvantage of the methods based on the measurement of power or current is that they cannot be used whenever the measurement of the source current is inaccessible or the loads are unidentified. In these cases, a control based on the measurement of the voltage at the PCC is preferable. This method draws on the basic consideration that a reduction of the voltage distortion at the PCC implies a reduction of the harmonic current of the grid [12]-[15]. In [15] the authors use the same principle but they compensate harmonics voltages of the grid by generating harmonic voltages with the active filter unit. The harmonic voltages to be generated are estimated by means of two possible methods, one iterative and one analytical based on the impedance of the grid. On the contrary, in the present paper, the voltage harmonics at the PCC are compensated injecting harmonic currents.

It is worth to note that if the voltage harmonics are not due to local non-linear loads but are present in the grid voltage, the power required for the compensation could exceed the available power of the converter. Thus, it would be necessary to estimate the grid impedance at a given frequency and to compensate only if this impedance is sufficiently high. The grid voltage harmonics can be discriminated by an on-line analysis of the spectrum of the impedance seen at the PCC [16]-[17]. However, in order to increase robustness, the control can be designed to not compensate or to compensate only partially the harmonics requiring too high power. As will be shown in the following, the control of each harmonic is based on a separated integral regulator. Thus, it is possible to limit the maximum action for each harmonic by introducing a saturation on each regulator. Moreover, if the saturation persists for a long time, the compensation of that harmonic can be stopped by setting to zero the corresponding regulator gain.

This paper proposes a method to compensate harmonics and inter-harmonics based on the measurement of the voltage directly at the terminals of the output-filter capacitors and not necessarily at the PCC. Therefore, the control is applicable also in case of RES far away from the PCC where the line impedance is not negligible. The effect of this line impedance connecting the converter to the PCC on the performances of the compensation is explicitly addressed.

The control is based on multiple reference frames (MRF) and includes an active damping for the mitigation of inter-harmonics, as proposed in [18]. The proposed control has been applied to a grid-tie converter for RES connected to a low voltage network with an ideal distorting load injecting harmonics and/or inter-harmonics. Experimental results on a laboratory setup have confirmed the validity of the theoretical methodology.

II. Review of algorithms for harmonic control based on voltage measurement

In early papers [19]-[20], the harmonic control has been addressed using resonant terms (selective controllers). This control method guarantees zero steady-state error at selected frequencies and allows adaptations to frequency variations. However, one resonant term must be designed and added for each harmonic to suppress, increasing the design effort. Furthermore, discrete time implementation of the algorithm presents difficulties, because the discretization method can produce poles outside the unity circle.

An alternative approach is represented by the repetitive controller that introduces a delay of one period of the fundamental grid frequency. Repetitive controllers resolve some issues of the selective controllers: the delays can be easily included in the discrete time and every harmonic within a specified bandwidth can be compensated for. However, repetitive controllers do not offer the possibility to compensate for single harmonic components or for specific subsets of harmonic components (e.g. compensate only the 5th, 11th and 17th while not compensating the 7th and the 13th). The latter problem has been addressed in [21] where the non-integer part of the repetitive controller delay is approximated by an adaptive filter to improve performance under variable frequency conditions.

The vector control is another common approach for harmonic compensation. Proportional + integral (PI) controllers in the synchronous reference frame (SRF) are frequently implemented in grid-tie converters, since each quantity varying at grid frequency appears as a constant at steady-state and, thus, PI control has zero static error [19]. However, harmonics are still seen as sinusoids in the fundamental SRF. Vector control can be enhanced using MRF [22]-[25], where the Park transformation is repeatedly applied to the space vector of the grid voltage using each time a SRF rotating at a different harmonic frequency. A PI controller can be designed independently for each harmonic with reference to the SRF rotating at the same frequency. This procedure is very attractive from the design point of view, but it has been considered excessively demanding from a computational perspective due to the large number of trigonometric functions to be calculated in real-time. Recently, a more computationally efficient implementation of the MSF-based control has been proposed in [25] and [26], where no trigonometric functions are calculated. This compensation method is used in this paper and complemented with an additional control loop for compensating inter-harmonics.

This article has been accepted for publication in a future issue of this journal, but has not been fully edited. Content may change prior to final publication. Citation information: DOI 10.1109/TIE.2016.2588462, IEEE Transactions on Industrial Electronics

III. CONTROL SCHEME AND REFERENCE CASE STUDY

As Fig. 1 shows, the grid-tie converter of the RES is connected to the PCC through a LC filter and a power line with non-zero impedance. A polluter injecting current harmonics and inter-harmonics is also connected to the PCC. The distorted currents can have different profiles and produce different distorted voltages at the PCC. Besides, the harmonic content of the voltage at the PCC can be also increased if the grid voltage is distorted.

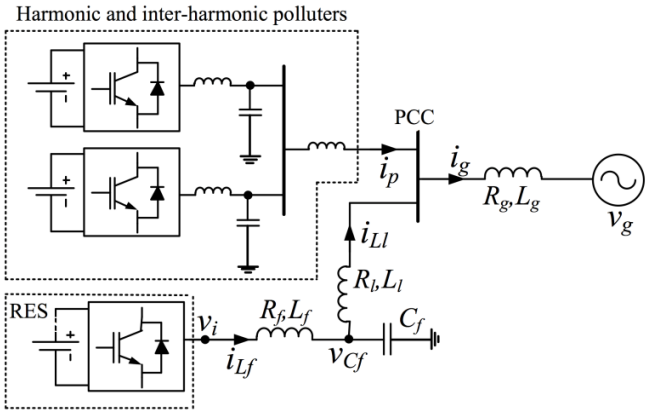

Fig. 1. Single-phase equivalent scheme of the case study

In Fig. 1, $\boldsymbol{v}_i$ is the converter voltage, $\boldsymbol{i}_{Lf}$ is the filter current, $\boldsymbol{v}_{Cf}$ is the voltage across the filter capacitor, $\boldsymbol{i}_g$ is the grid current, $\boldsymbol{i}_{Ll}$ is the line current, $\boldsymbol{i}_p$ is the current polluted with harmonic injected into the PCC, $\boldsymbol{v}_s$ is the grid voltage, R_f, L_f and C_f are the parameters of the LC filter, R_l and L_l are the equivalent resistance and inductance of the line and R_g and L_g are the equivalent resistance and inductance of the grid. Boldface letters are used for vectors.

The aim of the proposed control is to ensure that the harmonic and inter-harmonic content of the PCC voltage is suppressed by removing the harmonics of the local capacitor voltage. The analysis is developed under the assumption that the distortion of the grid voltage has been identified and the relative harmonics are excluded from the compensation algorithm. As Fig. 2 shows, the proposed control scheme includes three controllers operating in the fundamental SRF that are detailed in the following sections.

A. Inner-current controller

The inner-current controller uses a PI regulator (see block "a" in Fig. 2) to control the output current of the converter $\boldsymbol{i}_{Lf}$. The model used to design this PI controller is:

$$\begin{bmatrix} I_{Lf,d}(s) \\ I_{Lf,q}(s) \end{bmatrix} = \begin{bmatrix} P_{1,d}(s) & P_{1,dq}(s) \\ P_{1,qd}(s) & P_{1,q}(s) \end{bmatrix} \begin{bmatrix} V_{i,d}(s) \\ V_{i,q}(s) \end{bmatrix} \quad (1)$$

where s is the Laplace-Transform variable, $P_{1,d}(s) = P_{1,q}(s)$, $P_{1,dq}(s) = -P_{1,qd}(s)$, and subscripts d and q indicate the Park transformation axes. Capital letters (e.g. $I_{Lf,d}$) are used not only for the Laplace Transform of the time domain variables (e.g. $\boldsymbol{i}_{Lf}$) but also for the transfer functions (e.g. $P_{1,d}$). The frequency response of $P_{1,d}(s)$ is used to set the gains of the PI controller. As the model is symmetric, these gains will be the same for the q axis. This inner-current controller includes the well-known decoupling terms required to avoid the cross coupling between d and q axes [27]. The resulting closed-loop transfer function can be written as:

$$F_{r1,d}(s) = \frac{I_{Lf,d}(s)}{I^*_{Lf,d}(s)} = \frac{P_{1,d}(s)\,C_d(s)}{1 + P_{1,d}(s)\,C_d(s)} \quad (2)$$

where $C_d(s)$ is the inner-current controller for the d axis.

It is worth to note that the output current of the converter and the grid current, respectively i_{Ll} and i_g, are not measured and that only i_{Lf} is measured for the inner control loop and for the protection of the converter itself. Implementing the proposed algorithm, the converter injects current harmonics to compensate voltage harmonics at the PCC.

The dc voltage on the bus capacitors has to be also actively controlled by means of the inverter connected to the grid. Indeed, this corresponds to ensuring the balance between the power supplied by the energy source connected on the dc bus and the power exchanged with the grid. The control of the dc voltage can be obtained acting on the first harmonic of the current and by means of a loopback chain on the square of the voltage as presented in [28].

B. Harmonic controller

An efficient multiple-reference-frame (EMRF) controller (see "b" in Fig. 2) whose implementation is described in [25]-[26], is used to compensate for the voltage harmonics at the PCC. MRF-based controllers can selectively treat each harmonic independently, choosing which harmonics will be compensated and which not. The number of reference frames is limited by the switching frequency of the converter. According to [29], the computational effort of this controller is very low because it can be implemented without evaluating any trigonometric functions. However, the number of frames should also consider the harmonics effectively present in the grid. Besides, if a reference frame is active but there is no such harmonic in the capacitor voltage, the output of the controller for that harmonic will be equal to zero.

According to the MRF technique [22], only the sine and cosine of the PLL angle have to be calculated. The rotation matrix $\boldsymbol{R}(n\theta)$ is used to calculate the error signal in each SRF and can be written as:

$$\mathbf{R}(n\theta) = \begin{bmatrix} \cos(n\theta) & \sin(n\theta) \\ -\sin(n\theta) & \cos(n\theta) \end{bmatrix} \quad (3)$$

where n is the harmonic order with respect to the fundamental SRF and θ is the phase angle obtained by the PLL. De Moivre formula is used to calculate the elements of this matrix and avoid the evaluation of trigonometric functions.

In order to ensure system stability, the design of the EMRF controller needs the frequency response at each targeted harmonic frequency of the closed-loop:

$$F_{r2,d}(s) = \frac{V_{Cf,d}(s)}{V^*_{Cf,d}(s)} = \frac{P_{2,d}(s)\,F_{r1,d}(s)}{1 + P_{2,d}(s)\,F_{r1,d}(s)} \quad (4)$$

where:

$$P_{2,d}(s) = \frac{V_{Cf,d}(s)}{I_{Lf,d}(s)} \quad (5)$$

This article has been accepted for publication in a future issue of this journal, but has not been fully edited. Content may change prior to final publication. Citation information: DOI 10.1109/TIE.2016.2588462, IEEE Transactions on Industrial Electronics

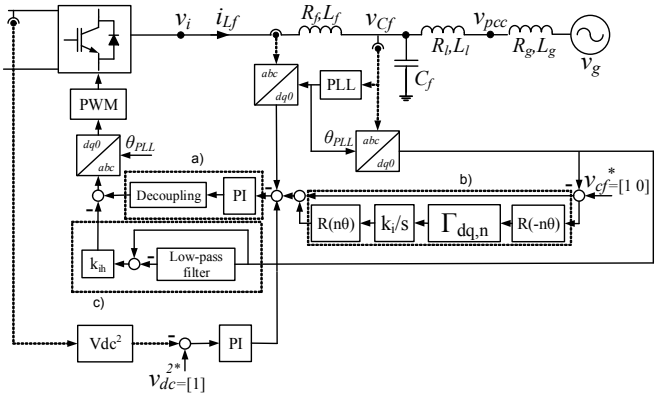

Fig. 2. Proposed control scheme: a) decoupled PI controller; b) EMRF controller; c) inter-harmonic controller

The inverse of this frequency response evaluated at each harmonic frequency is used in the block indicated with $\mathbf{\Gamma}_{dq,n}$ in Fig. 2. It should be noted that $\mathbf{\Gamma}_{dq,n}$ is a 2x2 matrix with constant coefficients which can be easily obtained during a preliminary commissioning stage by using the same MRF created for the harmonic controller. Consequently, this matrix will also compensate real-time issues such as discrete-time delays and dead-time.

At commissioning stage, a step is applied to the *d* axis of the control signal for each SRF, producing a sinusoidal signal for each harmonic in the fundamental SRF. This signal is applied to the controller and produces a steady-state error. It is worth to note that this is not an integral part of the control in normal conditions but is used only for characterizing and compensating the open loop behavior. Thus, this operation could be repeated several times during the lifetime to compensate mistuning or parametric changes due to aging. Finally, using the steady state error signal and the control signal in each SRF, which are constant values, the frequency response at each harmonic frequency is determined.

The open-loop transfer function used to design this controller is shown in Fig. 3 and can be written as:

$$G_d(s)=\frac{U'_d(s)}{U_d(s)}=-F_{r2,d}(s)\,C_{sel,d}(s) \tag{6}$$

where $C_{sel,d}(s)$ is the equivalent resonant controller of the EMRF controller in the fundamental SRF [26] and the main controller in Fig. 3 is the inner-current controller of Fig. 2, block "a". If the identification is perfectly implemented, the phase margins of $G_d(s)$ will be 90° (see Fig. 4).

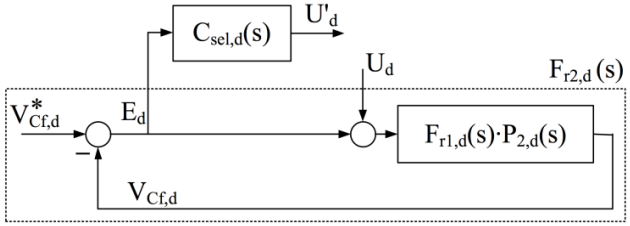

Fig. 3. Block diagram of the open-loop transfer function $G_d(s)$

The "plug-in" structure of the EMRF controller produces an open-loop frequency response $G_d(s)$ with the shape of a low-pass filter, which is related to the closed-loop frequency response $F_{r1,d}(s)$ obtained by the decoupled PI controller. Therefore, the higher the ultimate frequency, the higher the gain margin. The same gain is used for every harmonic in order to maintain this relationship. Accordingly, only a single gain k_i must be designed.

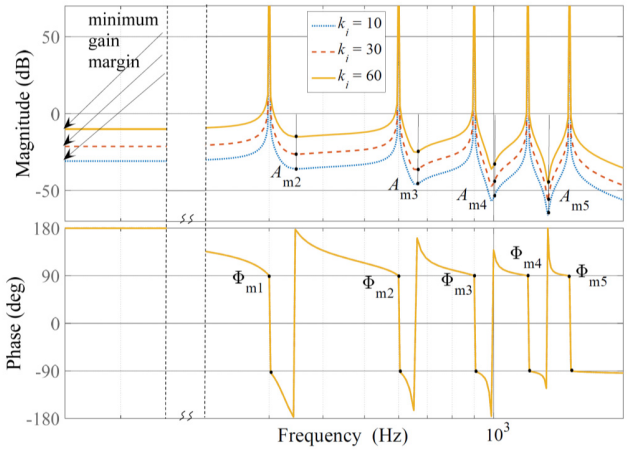

Fig. 4. Bode diagram of the opposite of the open-loop transfer function $-G_d(s)$

Fig. 4 shows the open-loop frequency response $G_d(s)$ for two different values of k_i. The minimum gain margin of $G_d(s)$ is at 0 Hz in the fundamental SRF, which corresponds to the fundamental frequency in the *abc* components. When the gain k_i increases, the gain margins A_{mk} decrease, while the phase margins Φ_{mk} are almost constant. Therefore, this controller can be designed like a proportional regulator: the higher the value of k_i, the lower the gain margin.

In addition, an integral action can also be included in the voltage controller to deal with fundamental frequency issues such as voltage sags/swells at the PCC. In any case, the *dq* set-point V_{Cf}* in p.u. is set to [1 0]. This means that the reference voltage V_{cf}* for the harmonics is set to zero except for the first harmonic that, as explained before, has to be controlled for balancing the dc bus voltage.

It should be noted that the proposed controller can easily select which harmonic to filter and which not. Indeed, setting k_i to zero for a specific harmonic will result in not compensating that harmonic.

C. Inter-harmonic controller

The third control loop is added in order to improve the performance of the proposed control strategy against inter-harmonics (see block "c" in Fig. 2). It consists of a proportional control, k_{ih}, in series to a high-pass filter (implemented using a low-pass filter in Fig. 2) in order to decrease the gain at every frequency except at the fundamental one of the disturbance-rejection-transfer functions, defined as:

$$F_{d1,d}(s)=\frac{V_{PCC,d}(s)}{I_{p,d}(s)};\quad F_{d2,d}(s)=\frac{V_{PCC,d}(s)}{V_{g,d}(s)} \tag{7}$$

Note that the module of $F_{d1,d}(s)$ and $F_{d2,d}(s)$ at the harmonic frequencies are already very low due to the EMRF controller. Therefore, this controller affects significantly only the frequencies different from the fundamental and the harmonics.

This article has been accepted for publication in a future issue of this journal, but has not been fully edited. Content may change prior to final publication. Citation information: DOI 10.1109/TIE.2016.2588462, IEEE Transactions on Industrial Electronics

With reference to Fig. 2, the open-loop transfer function used to design this controller can be written as:

$$G_{ih,d}(s) = \frac{F_{r1,d}(s)\,P_{2,d}(s)\,C_d(s)\,k_{ih}}{1 + F_{r1,d}(s)\,P_{2,d}(s)\,C_d(s)\left[1 + C_{sel,d}(s)\right]} \quad (8)$$

where k_{ih} is the proportional gain of the inter-harmonic controller. Fig. 5 shows the open-loop frequency response $G_{i,d}(s)$ for two different values of k_{ih}. Moreover, Fig. 6 shows how the inter-harmonic control affects the closed-loop frequency response $F_{d1,d}(s)$.

As shown in Fig. 6, the inter-harmonic controller reduces the gain at the inter-harmonic frequencies. Therefore, the performance of the system against inter-harmonic is improved.

IV. Effect of the Line and Grid Impedances on the Harmonic and Inter-Harmonic Compensation

The impedance of the line between the converter and the PCC reduces the harmonic compensation capabilities of the controller, because the voltage at the PCC is not equal to the voltage across the filter capacitors. This section studies the relationships between the magnitude of the impedances of the line and the grid and the attenuation of the harmonic and inter-harmonic content of the PCC voltage in order to determine when it is beneficial to compensate for the voltage harmonics across the filter capacitors.

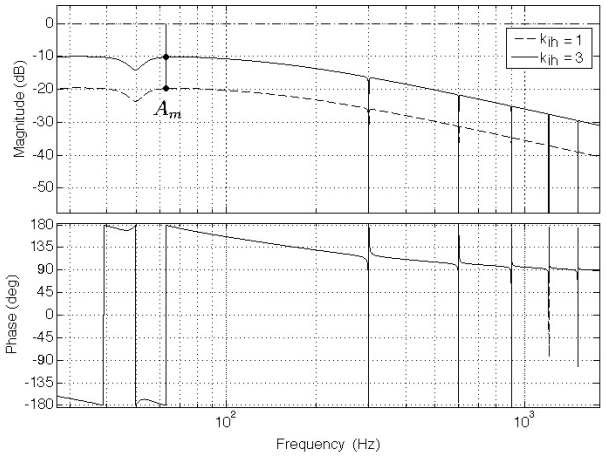

Fig. 5. Bode diagram of the open-loop transfer function $G_{ih,d}(s)$

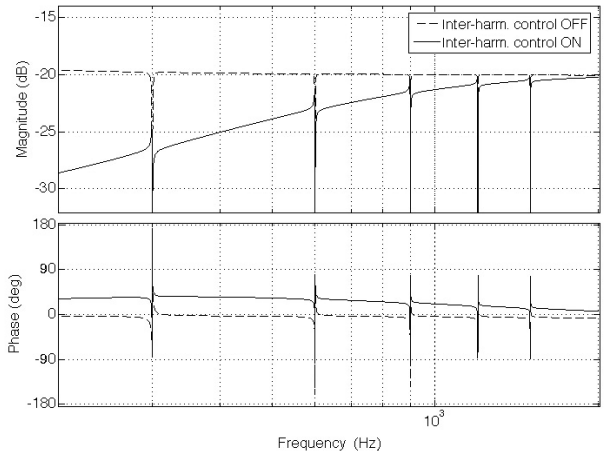

Fig. 6. Bode diagram of the closed-loop transfer function $F_{d1,d}(s)$ without and with inter-harmonics

A. Effect on the harmonic compensation

The harmonic content of the PCC voltage and the grid currents without the proposed harmonic control can be analysed with the equivalent circuit of Fig. 7a. It should be noted that $\boldsymbol{i}_{Ll}$ is the current across the line connecting the converter to the PCC. In this analysis, the current $\boldsymbol{i}_{Lf}$ is considered as an ideal current source as the inner-current controller typically has a wide bandwidth.

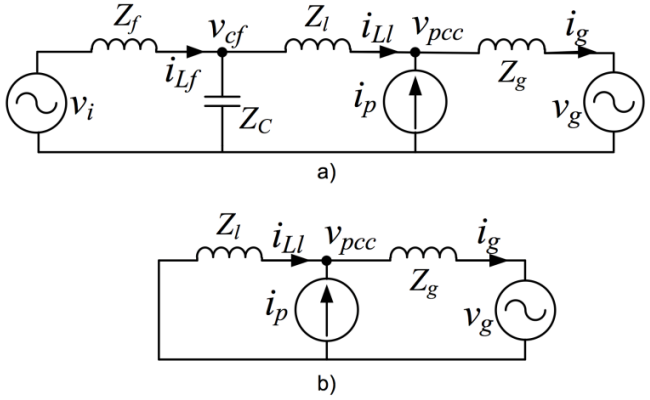

Fig. 7. Scheme of the models used in this analysis.

Using the superposition principle for each harmonic, the equation that describes the relationship between $\boldsymbol{v}_{pcc}$ and the disturbances $\boldsymbol{i}_p$ and $\boldsymbol{v}_g$ can be written as:

$$\mathbf{v}_{\mathrm{pcc}} = \mathbf{i}_{\mathrm{Lf}}\frac{Z_c\,Z_g}{Z_c+Z_l+Z_g} + \mathbf{i}_{\mathrm{p}}\frac{(Z_c+Z_l)\,Z_g}{Z_c+Z_l+Z_g} - \mathbf{v}_{\mathrm{g}}\frac{Z_c+Z_l}{Z_c+Z_l+Z_g} \quad (9)$$

Similarly, the equations that describe the relationship between $\boldsymbol{i}_g$ and the disturbances $\boldsymbol{i}_p$ and $\boldsymbol{v}_g$ can be written as:

$$\mathbf{i}_{\mathrm{g}} = \mathbf{i}_{Lf}\frac{Z_c}{Z_c+Z_l+Z_g} + \mathbf{i}_{\mathrm{p}}\frac{Z_c+Z_l}{Z_c+Z_l+Z_g} - \mathbf{v}_{\mathrm{g}}\frac{1}{Z_c+Z_l+Z_g} \quad (10)$$

When the proposed control strategy is used, the capacitor voltage of the filter has no harmonic content. Therefore, the harmonic content of the PCC voltage and grid current can be studied with the reduced model of Fig. 7b. Using again the superposition principle, it is possible to write:

$$\mathbf{v}_{\mathrm{pcc}} = \mathbf{i}_{\mathrm{p}}\frac{Z_l\,Z_g}{Z_l+Z_g} - \mathbf{v}_{\mathrm{g}}\frac{Z_l}{Z_l+Z_g} \quad (11)$$

and:

$$\mathbf{i}_{\mathrm{g}} = \mathbf{i}_{\mathrm{p}}\frac{Z_l}{Z_l+Z_g} - \mathbf{v}_{\mathrm{g}}\frac{1}{Z_l+Z_g} \quad (12)$$

Equations (9), (10), (11) and (12) correlate voltage and current variables. Superposition can be applied in order to obtain relationships between only two variables, making zero the rest of them:

$$\frac{\mathbf{v}_{\mathrm{pcc}}}{\mathbf{v}_{\mathrm{g}}} = -\frac{\mathbf{i}_{\mathrm{g}}}{\mathbf{i}_{\mathrm{p}}} = \frac{\mathbf{v}_{\mathrm{pcc}}}{\mathbf{i}_{\mathrm{p}}Z_g} \quad (13)$$

The effect on the harmonic compensation is analysed for different X_l / R_l ratios, where $X_l = \omega L_l$ is the line reactance and ω is the angular frequency of the grid. For low-voltage distribution networks, the resistance of the line is usually higher than the reactance, because the line is often a cable.

Fig. 8 shows the relationships described in (13) for both models (see Fig. 7a and Fig. 7b) when the line reactance varies

This article has been accepted for publication in a future issue of this journal, but has not been fully edited. Content may change prior to final publication. Citation information: DOI 10.1109/TIE.2016.2588462, IEEE Transactions on Industrial Electronics

for a X_l / R_l ratio equal to 2 at 50 Hz. As shown in Fig. 8, the harmonic level is lower with the proposed control up to a critical value of the line reactance. The higher the harmonic to compensate for, the lower the value of the critical line reactance $X_{l,rit}$. For example, the critical line reactance for the 30th harmonic is 0.011 p.u. Therefore, for each given value of the line reactance, there is a maximum filterable harmonic content above which the controller should not be used.

Table I shows the variation of the critical line reactance for different harmonics and different X_l / R_l ratios. The critical line reactance increases generally for smaller ratios.

Finally, the effect of the grid inductance has been investigated. The short circuit ratio of the grid X_g / R_g is set to 10, where $X_g = \omega L_g$. Table II shows the values of the critical line reactance for different harmonics when the grid reactance is changed. The critical line impedance is slightly increasing when the grid impedance is strongly decreasing. This means that the grid impedance has a very small impact on the critical line impedance.

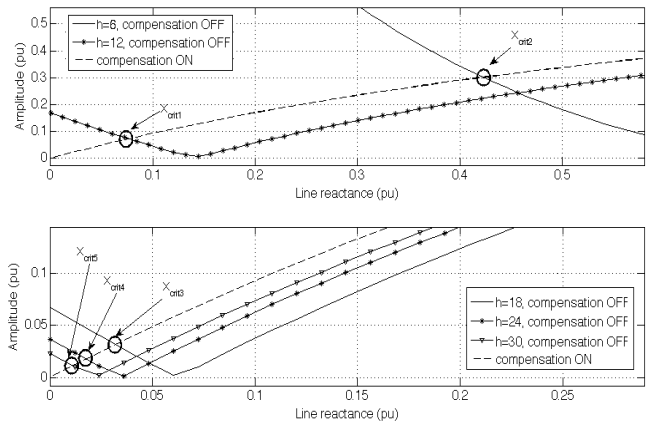

Fig. 8. Harmonic level in the relationships described in (13) with and without the proposed control

In summary, even if a rough estimation of the line impedance is available, it is possible to determine up to which harmonic of the local capacitor voltage should be compensated in order to ensure that the THD at the PCC voltage is always reduced.

TABLE I: CRITICAL LINE REACTANCE FOR DIFFERENT X_L/R_L RATIOS.

Harmonic	$X_l / R_l = 2$	$X_l / R_l = 0.5$	$X_l / R_l = 0.2$
6	0.412 pu	0.443 pu	0.679 pu
12	0.086 pu	0.087 pu	0.088 pu
18	0.032 pu	0.032 pu	0.032 pu
24	0.018 pu	0.018 pu	0.018 pu
30	0.011 pu	0.011 pu	0.011 pu

TABLE II: CRITICAL LINE REACTANCE FOR DIFFERENT GRID IMPEDANCES.

Harmonic	$X_g = 1$pu	$X_g = 0.1$pu	$X_g = 0.01$pu
6	0.412 pu	0.434 pu	0.445 pu
12	0.086 pu	0.115 pu	0.12 pu
18	0.032 pu	0.041 pu	0.047 pu
24	0.018 pu	0.021 pu	0.025 pu
30	0.011 pu	0.013 pu	0.018 pu

B. Effect on the inter-harmonic compensation

The equivalent model shown in Fig. 7a can be used for the inter-harmonic frequencies with and without the inter-harmonic controller as no integrator is used in the inter-harmonic controller.

According to Fig. 6, the inter-harmonic controller is improving the disturbance-rejection frequency response for inter-harmonic frequencies. The inter-harmonic compensation capability is only limited by the bandwidth of the controller. This effect is independent on the line and grid impedances, as the inter-harmonic compensation is only proportional to the inter-harmonic magnitudes of the local capacitor voltage.

V. SIMULATION RESULTS

The performance of the proposed control strategy has been verified by numerical simulations of the system represented in Fig. 1 for a power of 60 kVA. The model is implemented in Matlab/Simulink and Simpower Systems toolbox.

TABLE III: PARAMETERS OF THE CASE STUDY

Rated power S_n	60 kVA
RMS grid voltage V_g	400 V
Grid frequency f	50 Hz
Filter inductance L_f	2 mH
Filter capacitor C_f	50 μF
Filter resistance R_{Lf}	62.8 mΩ
Grid inductance L_g	1 mH
DC link voltage V_{DC}	700 V

The parameters used for the case study of the simulation are reported in Table III.

In the following, all the quantities will be analysed in per unit. The base values are 60 kVA for the power, 400 V for the voltage and 50 Hz for the frequency. In this first scenario, the grid voltage is purely sinusoidal and, hence, the distortion at the PCC is produced only by the non-linear current $\boldsymbol{i}_p$ absorbed by the polluter converter. The polluter is a converter controlled to absorb the current harmonics of a load connected via a diode rectifier. The output current of this converter is controlled to track the harmonic and inter-harmonic references with the same control scheme depicted in Fig. 2. The inverter-switching frequency and the control-sampling frequency are set to 10 kHz for the converter of the RES and the polluter.

The proportional and integral gains of the PI controller are $k_p = 0.5$ and $T_i = 65$ s respectively. The design procedure is carried out by selecting the closed-loop poles of the plant with the PI controller and then calculating the values of the gains. The damping coefficient of the closed-loop poles has been chosen equal to 0.707 and the settling time has been chosen equal to 4 ms. The EMRF controller is configured to reject $|1 \pm 6k|$ harmonics where $k = 1, 2 \ldots 5$ to show the effectiveness of the proposed controller in harmonic compensation. However, the number of the harmonics to be tracked will be different in the next section, where the line impedance between the PCC and the capacitor filter will be considered. The commissioning stage has been carried out to obtain the frequency response at each harmonic. As commented in

This article has been accepted for publication in a future issue of this journal, but has not been fully edited. Content may change prior to final publication. Citation information: DOI 10.1109/TIE.2016.2588462, IEEE Transactions on Industrial Electronics

Section III, after this step, only the gain k_i must be set to design the EMRF controller. The gain k_i used for the harmonic controller is chosen equal to 60 to obtain a minimum gain margin equal to 10dB, according to Figure 4.

A. Harmonic compensation of the PCC voltage

The polluter converter has been configured to inject a harmonic current, as depicted in Fig. 9. The line impedance Z_l has been set equal to zero. Fig. 9 also shows the transient response of the PCC voltage and the grid current when the proposed controller is turned on at 0.02 seconds.

The compensation for the harmonic content of the PCC voltage reduces the THD of the grid current from 35.5% to 0.73%. The controller has a transient response of two cycles of the fundamental frequency. In this case, the compensation is almost perfect as the line impedance is equal to zero.

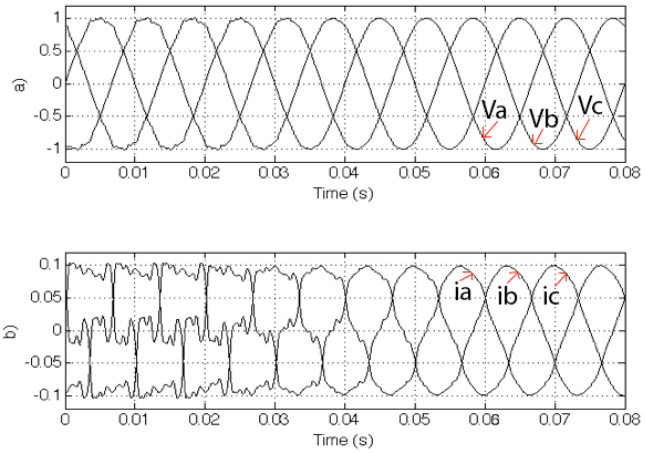

Fig. 9. Transient response when the proposed control is turned on: a) PCC voltage (in p.u.), b) grid currents (in p.u.)

As commented in Section IV, the performance of the harmonic compensation is reduced when there is a line impedance, because it is not possible to measure the harmonic content of the PCC voltage. In order to illustrate this result, the polluter is configured to inject the 11th harmonic into the PCC. From Table I, the critical reactance for this harmonic is 0.115 p.u. (0.34 Ω). Fig. 10 shows the magnitude of the 11th harmonic of the grid current before and after the activation of the proposed controller for two different values of the line reactance.

As predicted by the theoretical analysis, the proposed controller reduces the magnitude of the harmonic only if the line reactance is below the critical value.

B. Inter-harmonic compensation of the PCC voltage

The polluter has been configured to inject an inter-harmonic having a frequency 5.5 times the fundamental frequency. As commented in Section III, only the gain k_{ih} must be chosen to design the inter-harmonic controller. By increasing the gain of the inter-harmonic controller, the inter-harmonic voltage components are reduced but the control can be unstable. For this reason, the gain has been designed with a trial and error procedure, resulting in a k_{ih} equal to 1.5, which is a good compromise between harmonic reduction and stability of the system.

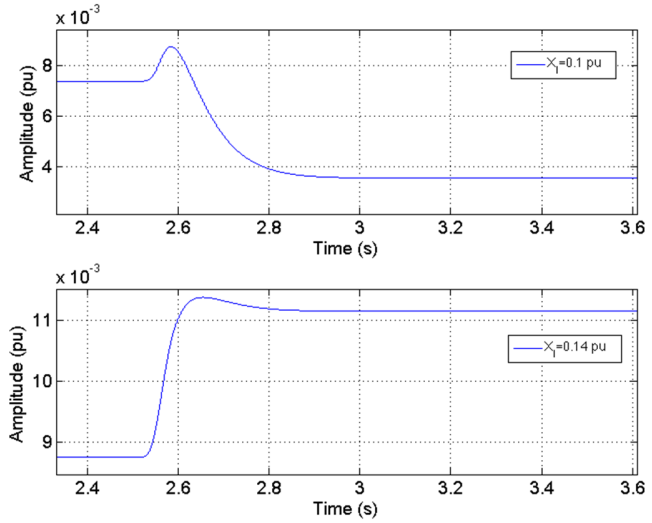

Fig. 10. 11th harmonic level in the grid currents when the line impedance is below and over the critical value

Fig. 11 shows that the magnitude of the inter-harmonic is significantly reduced when the controller is turned on. The dynamic response of the compensator is not shown in the figure because the inter-harmonic compensation is 10 times slower than the harmonic compensation.

VI. Experimental Results

A 60 kVA experimental setup with three voltage source converters has been assembled as shown in Fig. 12. One converter simulates the generating source, while the other two converters are the polluters generating harmonics and inter-harmonics. The real-time controller of the converters is based on an Opal RT system with a control step of 100 µs and switching frequency of 10 kHz. The base values are the same used for the simulations. The nominal RMS voltage at the PCC, the grid frequency, the DC voltage and the parameters of the filter are the same of the simulations. The line inductance is L_l = 0.3 mH (0.0294 pu). Since the characteristic of the real grid is equal to those of the simulated one, all the controller parameters have been chosen equal to those used for the simulations.

A. Experimental results for the harmonic compensation

In this experiment, the polluter converter injects the 5th, 7th, 11th, 13th and 17th harmonics with amplitude of 4%, 2%, 3%, 2% and 1% of the fundamental harmonic, respectively. The ratio of these harmonics represents the typical current absorption of a diode rectifier while their absolute amplitudes have been chosen in order to avoid the saturation limits of the power converter that acts as the polluter. The highest order harmonic current injected by the polluter, the 17th, is limited by the switching frequency of the polluter. Besides, the grid voltage contains 5th and 7th harmonic. Therefore, both the PCC voltage and the local capacitor voltage are used to show the effectiveness of the proposed control. Fig. 13 shows the transient response of the local capacitor voltage when the proposed controller is turned on at t = 0 s.

This article has been accepted for publication in a future issue of this journal, but has not been fully edited. Content may change prior to final publication. Citation information: DOI 10.1109/TIE.2016.2588462, IEEE Transactions on Industrial Electronics

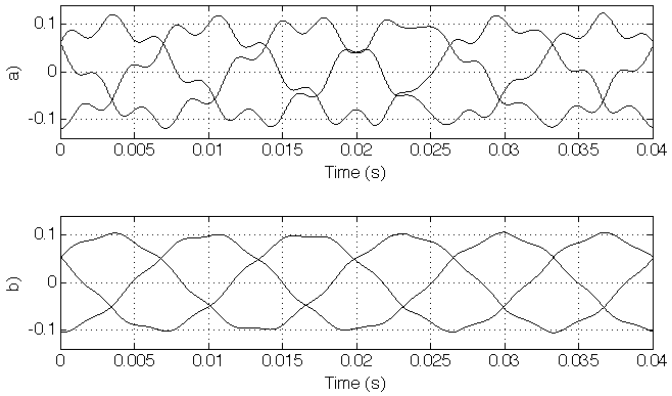

Fig. 11. Grid currents at steady-state (in p.u.): a) without inter-harmonic controller, b) with inter-harmonic controller

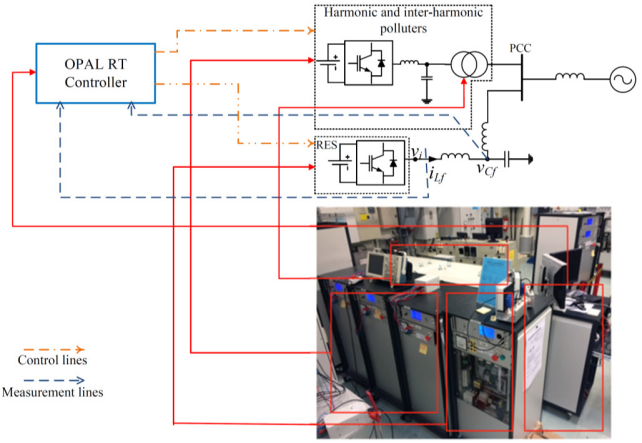

Fig. 12. Picture of the laboratory prototype used for the experiments.

Similarly to the simulated results shown in Fig. 9, the transient vanishes within a cycle of the fundamental frequency. Besides, the THD at steady-state of the local capacitor voltage is 0.99%. Fig. 14 shows that at steady-state the harmonic content of the PCC voltage is significantly improved with the proposed controller, while the local capacitor voltage is perfectly compensated.

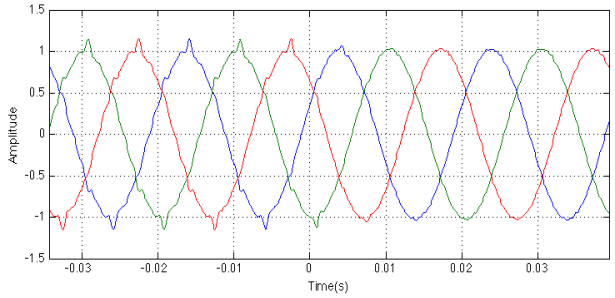

Fig. 13. Transient response of the local capacitor voltage (in p.u.) before and after switching on the harmonic controller

The same experiment has been repeated with a line inductance of 1.3 mH (0.127 pu), which has been selected to have some of the harmonics above the critical value. For a so high line reactance, according with Table I and with eq. (13) it should be better not to compensate for any harmonic equal or higher than the 11th.

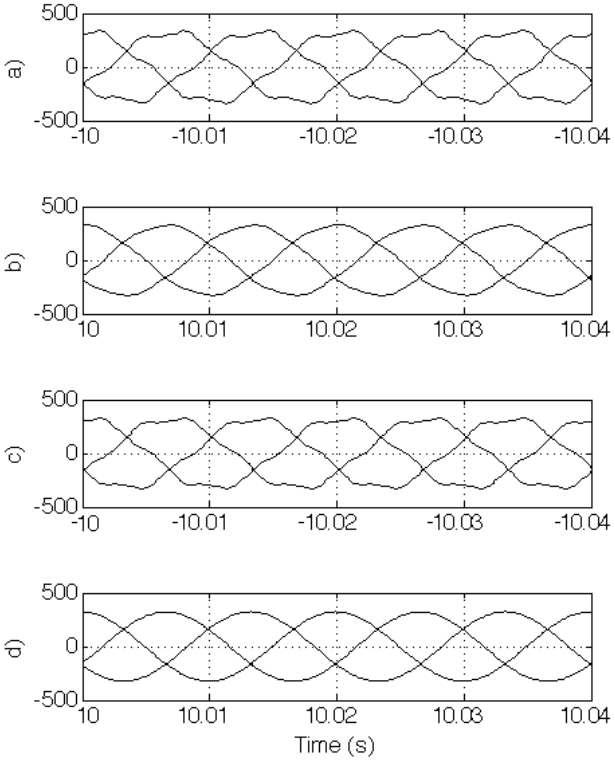

Fig. 14. Steady-state response before and after the harmonic controller is switched on (in p.u.): a) v_{PCC} before, b) v_{PCC} voltage after, c) v_{Cf} before, d) v_{Cf} after

A compensation of harmonics whose order is greater than 11th will lead to an increase of the harmonic for the presence of the high line inductance. Also if the compensation could be avoided just setting to zero the regulator constants, in order to highlight the correctness of what discussed in section IV.A the test has been performed both with compensation and without compensation of 11th, 13th, 17^{h} and 19th harmonics. Fig. 15 shows that the harmonics 11th, 13th, 17^{h} and 19th are increased when the harmonic controller is turned on.

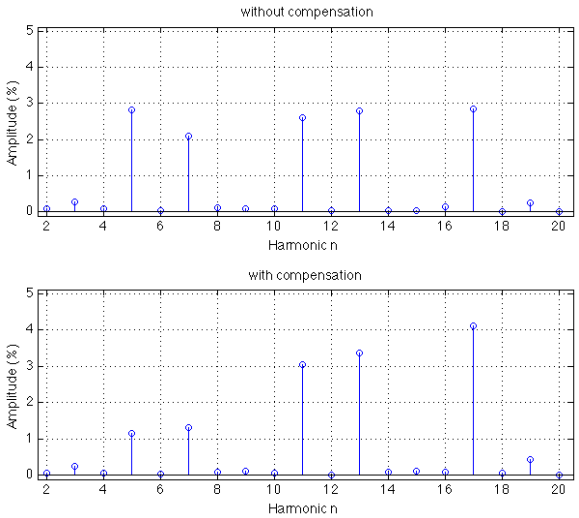

Fig. 15. Spectrum of the PCC voltage as percentage of first harmonic without and with the proposed harmonic controller.

This article has been accepted for publication in a future issue of this journal, but has not been fully edited. Content may change prior to final publication. Citation information: DOI 10.1109/TIE.2016.2588462, IEEE Transactions on Industrial Electronics

In this case only the harmonics 5th and 7th should be compensated to ensure a reduction of the THD at the PCC voltage. The THD before the compensation is 6.13 % and after the compensation is 6.42 %. If the harmonics 11th, 13th, 17th and 19th are not compensated, the THD decreases to 5.06%.

B. Experimental results for inter-harmonics compensation

In this experiment, the polluter converter injects also an inter-harmonic at 5.5 times the fundamental frequency. Fig. 16 shows the steady-state response before and after the harmonic and inter-harmonic controllers turn on. The inter-harmonic magnitude of the PCC voltage before and after is 3.48% and 1.03% respectively.

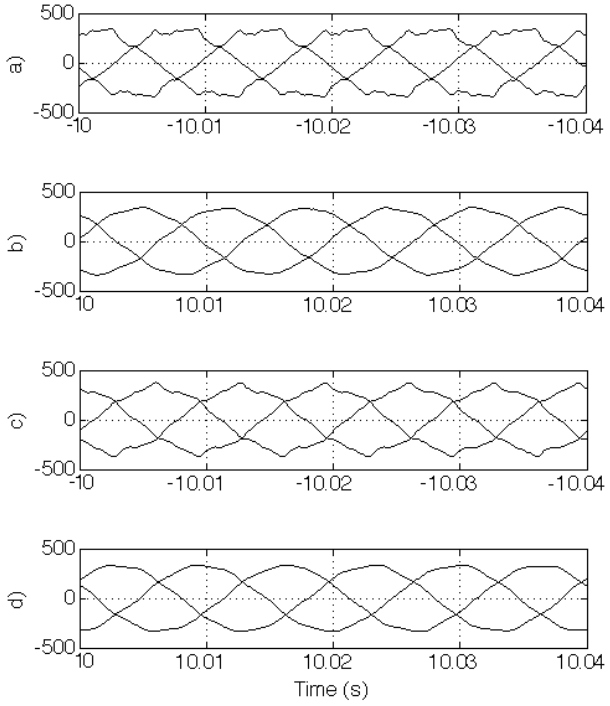

Fig. 16. Steady-state response without and with the harmonic and inter-harmonic controller (in p.u.):: a) v_{PCC} before, b) v_{PCC} voltage after, c) v_{Cf} before, d) v_{Cf} after

VII. CONCLUSION

A harmonic and inter-harmonic controller for grid-tie converters for renewable energy sources has been proposed in this paper. The control is based only on the measurement of the voltage across the filter capacitor, which is recommended when the load or grid current is not available. Both harmonic and inter-harmonic controllers are very easy to design, as only two gains have to be selected. Two scenarios have been considered for the analysis of the compensation capabilities of the proposed controller. In the first scenario the impedance between the local capacitor and the PCC is almost zero and the compensation of the harmonics and inter-harmonics is improved for all considered frequencies. In the second scenario the impedance between the local capacitors and the PCC is not negligible and sets an upper limit for the order of harmonic to compensate. Experimental results have validated the very good performance of the proposed controller against the compensation for harmonics and inter-harmonics. Besides, further experiments have confirmed the existence of a critical value of the line impedance that has an influence on the performance of the proposed controller. Finally, it has been experimentally verified that the harmonic compensation service can be offered with a low impact on the amount of generable power. In the cases analysed in the paper, the impact on the power generated by the renewable source is between 5% and 15%, depending on the number of harmonics that are compensated.

REFERENCES

[1] IEEE Recommended Practices and Requirements for Harmonic Control in Electrical Power Systems, *IEEE Std. 519-2014*, 2014.

[2] B. Saint, "Rural distribution system planning using Smart Grid Technologies," *IEEE Rural Electric Power Conference*, 2009. REPC '09, pp. B3,B3-8, 26-29 April 2009.

[3] T.T. Erbato, T. Hartkopf, "Smarter Micro Grid for energy solution to rural Ethiopia," *IEEE PES Innovative Smart Grid Technologies (ISGT)*, pp.1,7, 16-20 Jan. 2012.

[4] J. H. R. Enslin and P. J. M. Heskes, "Harmonic interaction between a large number of distributed power inverters and the distribution network", *IEEE Trans. Power Electron.*, vol. 19, no. 6, pp. 1586,1593, Nov. 2004.

[5] M. Brenna, G. C. Lazaroiu, G. Superti-Furga and E. Tironi, "Bidirectional Front End Converter for DG with Disturbance Insensitivity and Islanding-Detection Capability", *IEEE Trans. Pow. Del.*, vol. 23, no. 2, pp. 907,914, Apr. 2008.

[6] T. N. Preda, K. Uhlen, D.E. Nordgård, "An overview of the present grid codes for integration of distributed generation," *Integration of Renewables into the Distribution Grid, CIRED 2012 Workshop*, pp.1,4, 29-30 May 2012.

[7] L W. Yun; J. He, "Distribution System Harmonic Compensation Methods: An Overview of DG-Interfacing Inverters," *IEEE Ind. Electron. Mag.*, vol.8, no.4, pp.18,31, Dec. 2014.

[8] S. Munir, L.W. Yun, "Residential Distribution System Harmonic Compensation Using PV Interfacing Inverter," *IEEE Trans. Smart Grid*, vol.4, no.2, pp.816,827, June 2013.

[9] L. Tzung-Lin, W. Yen-Ching, L. Jian-Cheng, "Design of a hybrid active filter for harmonics suppression in industrial facilities," *International Conference on Power Electronics and Drive Systems*, 2009. PEDS 2009, pp.121,126, 2-5 Nov. 2009.

[10] Wind Energy Center, University of Massachusetts Amherst, "Wind Power: Capacity Factor, Intermittency, and what happens when the wind doesn't blow?", Community Wind Power Fact Sheet 2a (http://www.leg.state.vt.us/jfo/envy/Wind%20Power%20Fact%20Sheet.pdf, accessed on February 6th, 2015)

[11] H. Sasaki and T. Machida, "A new method to eliminate AC harmonic currents by magnetic compensation - considerations on basic design", *IEEE Trans. Power App. Sys.*, vol. 90, no. 5, pp. 2009,2019, Sep. 1971.

[12] M. El-Habrouk, M. K. Darwish and P. Mehta, "Active power filters: a review," *IEE Proceedings - Electric Power Applications*, vol. 147, no. 5, pp. 403,413, Sep 2000.

[13] G. Angeli, G. Superti-Furga, and E. Tironi, "Harmonic Damping by Means of DG Front-End Converter. Part I: Theory and Algorithm", *Proc. 13th Int. Conf. Harmonics and Quality of Power ICHQP 2008*, pp. 1,5, Wollongong, Australia, 28 Sep.-1 Oct. 2008.

[14] S. D'Arco, L. Piegari, P. Tricoli, "Harmonic compensation with active front-end converters based only on grid voltage measurements," *3rd Renewable Power Generation Conference (RPG 2014)*, pp.1,6, 24-25 Sept. 2014.

[15] D. Menniti, A. Burgio, N. Sorrentino, A. Pinnarelli, "Implementation of the shunt harmonic voltages compensation approach", *Elsevier Electric Power Systems Research*, vol. 81, no. 3, pp. 798,804, March 2011.

[16] L. Asiminoaei, R. Teodorescu, F. Blaabjerg, U. Borup, "Implementation and Test of an Online Embedded Grid Impedance Estimation Technique for PV Inverters," *IEEE Trans. Ind. Electron.*, vol.52, no.4, pp.1136,1144, Aug. 2005.

[17] S. Cobreces, E.J. Bueno, D. Pizarro, F.J. Rodriguez, F. Huerta, "Grid Impedance Monitoring System for Distributed Power Generation Electronic Interfaces," *IEEE Trans. Instrum. Meas.*, vol.58, no.9, pp.3112,3121, Sept. 2009.

[18] D. Basis, V.S. Ramsden and P.K. Mutik "Hybrid filter control system with adaptive filters for selective elimination of harmonics and interharmonics," *IEE Proc. Electric Power Applications.*, vol. 147, no. 3, pp. 295,303, Jul 2000.
[19] D.N. Zmood, D.G. Holmes, "Stationary frame current regulation of PWM inverters with zero steady-state error", *IEEE Trans. on Power Electron.*, Vol. 18, no. 3, pp. 814,822, May 2003.
[20] M.J. Newman, D.N. Zmood, D.G. Holmes, "Stationary frame harmonic reference generation for active filter systems", *IEEE Trans. Ind. Appl.*, Vol. 38, no. 6, pp. 1591,1599, Dec. 2002.
[21] J. Roldan-Perez, A. Garcia-Cerrada, J.Z. Zamora-Macho, P. Roncero-Sanchez, E. Acha, "Adaptive repetitive controller for a three- phase dynamic voltage restorer, *III International Conference on Power Engineering, Energy and Electrical Drives (IEEE POWERENG 2011)*, pp. 1,6, May 2011.
[22] S.J. Lee and S.-K. Sul., "A harmonic reference frame based current controller for active filter" *Proc. Applied Power Electronics Conference (APEC)*, pp. 1073,1078, Feb. 2000.
[23] P. Mattavelli, "A closed-loop selective harmonic compensation for active filters" *IEEE Trans. Ind. Appl.*, Vol. 37, no. 1, pp. 81,89, Jan/Feb 2001.
[24] D.N. Zmood, D.G. Holmes, and G.H. Bode, "Frequency-domain analysis of three-phase linear current regulators" *IEEE Trans. Ind. Appl.*, Vol. 37, no.2, pp. 601,610, March/April 2001.
[25] M. Ochoa-Gimenez, J. Roldan-Perez, J.L. Zamora-Macho, A. Garcia-Cerrada, "Space-vector-based controller for current-harmonic suppression with a shunt active power filter" *European Power Electronics and Applications Journal – EPE Journal*, vol.24, no 2, April 2014.
[26] F. Shahnia, S. Rajakaruna, A. Ghosh, "Static compensators (STATCOMs) in power systems", ISBN 978-981-287-281-4, *Springer*, 2015.
[27] B. Bahrani, A. Karimi, B. Rey, A. Rufer, "Decoupled dq-current control of grid-tied voltage source converters using nonparametric models", in *IEEE Trans. Ind. Electron.*, vol. 60, no. 4, pp. 1356,1366, April, 2013.
[28] S. Grillo, V. Musolino, L. Piegari, E. Tironi, C. Tornelli, "DC Islands in AC Smart Grids", *IEEE Trans. Power Electron.*, vol. 29, no. 1, pp. 89,98, Jan. 2014.
[29] M. Ochoa-Giménez, J. Roldán-Peréz, A. García-Cerrada, J. L. Zamora-Macho, "Efficient multiple-reference-frame controller for harmonic suppression in custom power devices", *Elsevier Electrical Power and Energy Systems*, vol. 69, pp. 344,353, July 2015.

Miguel Ochoa Giménez was born in Madrid, Spain in 1986. In 2011, he obtained the degree of Engineering in Automatics and Electronics at Comillas Pontifical University in Madrid. He obtained the Master in Research in Engineering Modelling Systems in 2013 and the International PhD with honors (Cum Laude) in 2015 both at Comillas Pontifical University.

He is working as Design Engineer at Gamesa Electric in Madrid. His areas of interest are FACTS, HVDC, VSC Control, Microgrids, Renewable Energy Integration and control systems.

Salvatore D'Arco received the M.Sc. and Ph.D.degrees in electrical engineering from the University of Naples Federico II, Naples, Italy, in 2002 and 2005, respectively.

He was, from 2006 to 2007, a Postdoctoral Researcher with the University of South Carolina, Columbia, SC, USA. In 2008, he joined ASML Holding N.V., Veldhoven, The Netherlands, where he worked as a Power Electronics Designer until 2010. From 2010 to 2012, he was a Postdoctoral Researcher with the Department of Electric Power Engineering, Faculty of Information Technology, Mathematics and Electrical Engineering, Norwegian University of Science and Technology, Trondheim, Norway. In 2012, he joined SINTEF Energy Research, Trondheim, Norway, where he currently works as a Research Scientist. He is the author of over 50 scientific papers, and he is the holder of one patent. His main research activities are related to the control and analysis of power electronic conversion systems for power system applications, including the real-time simulation and rapid prototyping of converter control systems.

Luigi Piegari (M'04-SM'13) was born in Naples, Italy, on April 2, 1975. He received the M.S. (cum laude) and Ph.D degrees in Electrical Engineering from the University of Naples Federico II, Italy, in 1999 and 2003, respectively.

He was, from 2003 to 2008, a Postdoctoral Research Fellow in the Department of Electrical Engineering, University of Naples Federico II, Italy. From 2009 to 2012, he was assistant professor at Department of Electrical Engineering of the Polytechnic University of Milan. He is currently associate professor of Electrical Machines and Drives at the Department of Electronics, Information and Bioengineering of the Polytechnic University of Milan. He is the author of more than 100 scientific papers published in international journals and conference proceedings. His research interests include storage devices modeling, wind and photovoltaic generation, modeling and control of multilevel converters and DC distribution grids.

Prof. Piegari is a member of the IEEE Industrial Electronics Society, of the IEEE Power Electronics Society and of AEIT. He is the Technical program Chair of the International Conference on Clean Electrical Power.

Pietro Tricoli (M'06) was born in Naples, Italy, on September 8, 1978. He received the M.S. (cum laude) and Ph.D. degrees in Electrical Engineering from the University of Naples Federico II, Italy, in 2002 and 2005, respectively.

He was a Visiting Scholar in the Department of Electrical and Computer Engineering, University of Wisconsin-Madison, Madison, in 2005. In 2006, he was also a Visiting Scholar in the Department of Electrical and Electronic Engineering, Nagasaki University, Nagasaki, Japan. From 2006 to 2011, he was a Postdoctoral Research Fellow in the Department of Electrical Engineering, University of Naples Federico II, Italy. He is currently a Lecturer of Electrical Power and Control in the Department of Electronic, Electrical, and Systems Engineering, University of Birmingham, Birmingham, U.K. He is the author of more than 60 scientific papers published in international journals and conference proceedings. His research interests include storage devices for road electric vehicles, railways, and rapid transit systems, wind and photovoltaic generation, railway electrification systems and modeling and control of multilevel converters.

Dr. Tricoli is a member of the IEEE Industrial Electronics Society and member of the IET Midlands Power Group. He is the Web & Publication Chair of the International Conference on Clean Electrical Power. He is a Registered Professional Engineer in Italy.